Available online at www.sciencedirect.com
SCIENCE DIRECT®
Lithos 70 (2003) 39–59
LITHOS
www.elsevier.com/locate/lithos

Origin of chromite in mafic–ultramafic-hosted hydrothermal massive sulfides from the Main Uralian Fault, South Urals, Russia

S.G. Tesalina[a,b], P. Nimis[b,*], T. Augé[c], V.V. Zaykov[a]

[a] *Institute of Mineralogy, Uralian Division, Russian Academy of Sciences, Miass 456301, Russia*
[b] *Dipartimento di Mineralogia e Petrologia, Università degli Studi di Padova, Corso Garibaldi 37, 35137 Padua, Italy*
[c] *BRGM, B.P. 6009, 45060 Orléans Cedex 2, France*

Received 21 November 2002; accepted 7 July 2003

Abstract

Mafic–ultramafic-hosted hydrothermal Fe–Cu–(Ni–Co) sulfide ores from the Main Uralian Fault Zone (MUFZ), South Urals (Ivanovka and Ishkinino ore fields), contain a relatively large (up to 3%) proportion of chromite. This association is common for magmatic Fe–Ni–Cu sulfides, but definitely unusual for hydrothermal sulfides. Textural, morphological and compositional data are used here to gain an insight into the origin and significance of this unusual chromite–sulfide association. The studied chromites occur both as broken fragments and as euhedral or subhedral crystals, which are included in the sulfides or scattered in their talc ± chlorite ± saponite ± quartz ± carbonate matrix. They are characterized by high Cr/(Cr + Al) ratios (0.58–0.85) and range in composition from magnesiochromite to chromite sensu stricto. Textural, morphological and compositional features, as well as the occurrence of relatively high-silica, low-Ti, low-K melt inclusions in some of the crystals, indicate that the ore-associated chromites (i) are a mixed population of grains derived from mafic–ultramafic mantle and crustal magmatic rocks and mantle peridotite melting residua, (ii) have no genetic relation with the host sulfides and (iii) represent relicts derived from the hydrothermally altered country rocks. The compositions of the chromites and of the melt inclusions denote a clear supra-subduction zone signature. The melts parent to the cumulitic chromites had an arc tholeiitic to, possibly, boninitic affinity. These data suggest that the host mafic–ultramafic complexes formed in an early arc or forearc setting and do not represent obducted portions of MORB oceanic lithosphere. Hence, contrary to previous interpretations, the associated massive sulfides could not originate on a mid-ocean ridge, but rather in an early arc or forearc environment. Given the relatively short life of the western Uralian arc system, the most probable time window for sulfide ore deposition is confined to Early to Middle Devonian time.

Keywords: Chromite; South Urals; Main Uralian Fault; VHMS deposits; Ivanovka; Ishkinino

1. Introduction

Chromite, including magnesiochromite and chromite sensu stricto, is a common accessory mineral in mafic and ultramafic rocks. By virtue of its compositional variability and sensitivity to the conditions of formation, chromite can serve as a useful petrological and geodynamic indicator (Dick and Bullen, 1984; Barnes and Roeder, 2001).

Elevated concentrations of chromite in igneous mafic–ultramafic complexes, also in the form of chromitites, are commonly associated with variable amounts of magmatic sulfides (e.g. Whitney and

* Corresponding author. Fax: +39-0498272010.
E-mail address: paolon@dmp.unipd.it (P. Nimis).

0024-4937/$ - see front matter © 2003 Published by Elsevier B.V.
doi:10.1016/S0024-4937(03)00090-2

Naldrett, 1989). Chromite deposits in mantle or mantle–crust transitional sections of supra-subduction zone (SSZ) ophiolites can be associated with hydrothermal, volcanic-hosted massive sulfide (hereafter VHMS) deposits occurring at upper volcanic levels (e.g. Yumul and Balce, 1994). Nonetheless, the occurrence of chromite within the VHMS ores is definitely rare. One such example is represented by the Cu–Co–Zn deposit of Outokumpu, Finland, where spinels characterized by strongly variable Cr, Al, Mg, Fe and Zn contents have been found both in the ores and in the hydrothermally altered, volcano-sedimentary country rocks (Treloar, 1987). Another example was reported by Candela et al. (1989), who described *detrital* chromite in the seafloor hydrothermal sulfide ores of the Sykesville District, Maryland Piedmont. More recently, Melekestseva et al. (2001) reported the occurrence of abundant chromite in the ultramafic-hosted hydrothermal sulfide mineralization of Ishkinino, Main Uralian Fault Zone (hereafter MUFZ), South Urals. Based on textural relations, Melekestseva et al. (2001) suggested a possible syngenetic relation between the chromites and the sulfides. If correct, this interpretation would imply a hydrothermal growth for the chromites. Although hydrothermal chromites are certainly unusual, mobilization of chrome by reducing, Cl-rich hydrothermal fluids has been proposed to explain the presence of volatile and sodium-rich fluid inclusions in some chromites from ophiolite complexes (Johan et al., 1983; Johan, 1986), the occurrence of chromite in some gold and sulfide deposits from the Urals and Soudan (Novgorod et al., 1984; Hottin and Aloub, 1990), and some of the compositional features of spinels from Outokumpu (Treloar, 1987).

Here, we aim to test the hypothesis of a hydrothermal genesis in the light of an extensive set of new analytical and textural data on sulfide-associated chromites from two VHMS deposits of the southern MUFZ. These include the Ishkinino deposit studied by Melekestseva et al. (2001) and a somewhat analogous occurrence located 55 km to the NNE near the village of Ivanovka (Fig. 1). The textural and compositional features of the chromites contained in the sulfides and in their host mafic and ultramafic rocks will be compared with those of worldwide chromites from different petrogenetic environments. The results will be used to discuss the origin and significance of chromites in the studied deposits and to gain an insight into the geodynamic setting of the host mafic–ultramafic massifs at the time of sulfide formation.

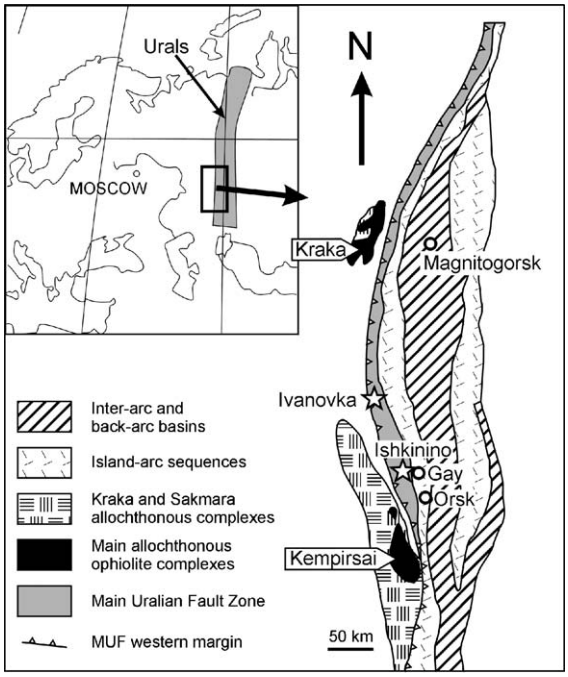

Fig. 1. Geological sketch map of the southern Urals, with location of the Ivanovka and Ishkinino ore fields.

2. Geological setting of the Ivanovka and Ishkinino deposits

The Urals are a linear orogenic belt that resulted from the Late Palaeozoic collision of the East European Platform with a Siberian–Kazakhian plate assemblage and interposed oceanic and island arc terranes. The suture zone between the colliding plates is marked by the MUFZ, a 2–10 km wide (locally up to 25 km wide), east-dipping fault system, which can be traced continuously along the Uralide orogen (e.g. Puchkov, 1997) (Fig. 1). In the south Urals, the MUFZ separates an accretionary wedge to the west, which carries slices of high-pressure metamorphic units of continental provenance (Maksyutov Complex), from a Late Emsian to Early Frasnian forearc–island arc complex (Magnitogorsk arc) to the east (Brown and Spadea, 1999). The earliest stage of the

Magnitogorsk arc development is marked by boninite-bearing arc-tholeiitic volcanism in its westernmost area (Baimak–Buribai region; Spadea et al., 1998), which was followed by arc-tholeiitic and low- to high-K calcalkaline volcanism (Maslov et al., 1993; Spadea et al., 2002). The MUFZ is interpreted as the main damage zone that developed along the arc backstop during Late Devonian collision of the Magnitogorsk arc with the East European continental margin (Brown and Spadea, 1999).

The MUFZ mainly consists of a mélange of serpentinites, derived from mantle harzburgites, less abundant dunites and minor lherzolites, with blocks of Ordovician to Middle Devonian volcanic and sedimentary rocks (e.g. Seravkin et al., 2001). Mafic–ultramafic complexes in the MUFZ are considered by a number of authors to be relicts of Silurian oceanic material (e.g. Zaykov et al., 2000a; Savelieva et al., 1997, 2002). A few of these complexes from the southern part of the MUFZ are host to subeconomic Fe–Cu–(Co–Ni) massive sulfide deposits, which include the Ivanovka and Ishkinino deposits studied in the present paper (Zaykov et al., 2000a; Tessalina et al., 2001; Herrington et al., 2002). These particular pyrrhotite-rich deposits are not typical for the Urals, where several examples of Cyprus-, Besshi-, Baimak-(Kuroko-) and Urals-type deposits occur (cf. Prokin and Buslaev, 1999; Herrington et al., 2002). Although the hydrothermal seafloor or subseafloor origin of the Ivanovka and Ishkinino deposits is supported by an increasing wealth of mineralogical and textural data, their significance is still debated and two contrasting paleogeodynamic environments, namely, a mid-ocean ridge and a forearc setting, have been proposed (Wipfler et al., 1999; Zaykov et al., 2000a,b; Tessalina et al., 2001; Nimis et al., in press). A description of main host-rock lithologies and ore facies of the two deposits is given below.

2.1. Ivanovka

The Ivanovka sulfide deposit is located near the east-dipping western margin of the MUFZ (Fig. 1). It consists of several, densely packed ore lenses and layers within a largely brecciated, up to 100–150 m thick mafic–ultramafic sequence (Buchkovskiy, 1970; Zakharov and Zakharova, 1975) (Fig. 2a). Main host-rock lithologies consist of extensively to completely hydrothermally altered mafic and ultramafic rocks, which included olivine-rich melagabbroids, gabbros,

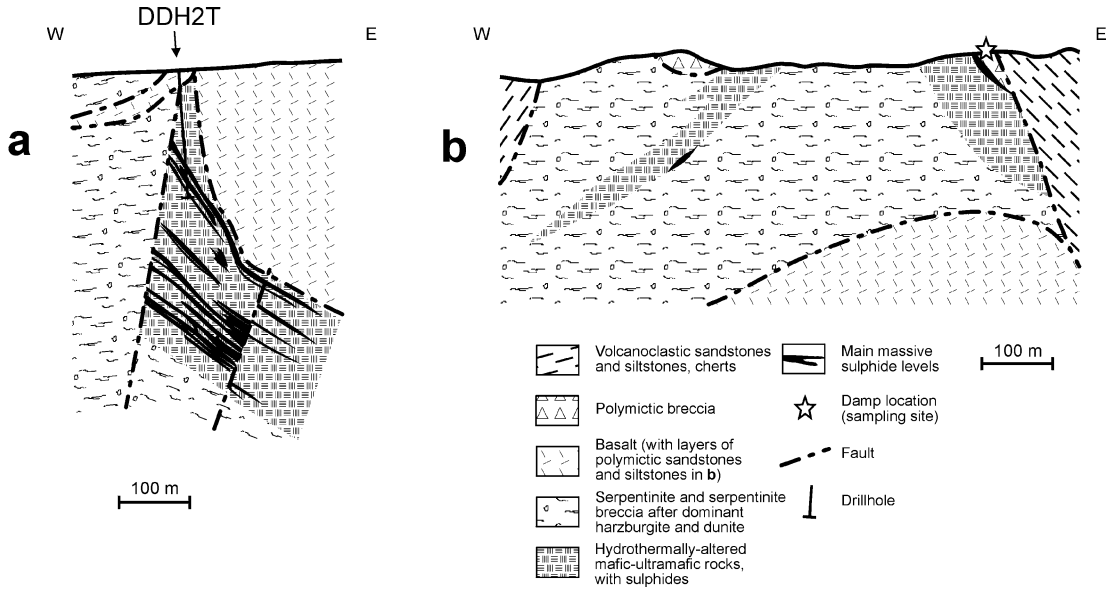

Fig. 2. (a) Geological section of the Ivanovka deposit (simplified after Buchkovskiy, 1970). (b) Geological section of the Ishkinino deposit (modified after Subbotin et al., unpublished work). Vertical distances to scale.

dolerites, basalts and mantle peridotites (Fig. 3). Hydrothermal alteration of these rocks produced various mineral assemblages depending on protolith composition and hydrothermal conditions. In particular, mafic protoliths were mostly transformed into chloritites, while ultramafic rocks and polymictic mafic–ultramafic breccias were dominantly transformed into talc ± Mg-rich chlorite ± carbonate ± (Mg, Si)-rich saponite (stevensite) ± quartz rocks (Nimis et al., in press). The sequence of ore-bearing, hydrothermally altered rocks lies between a footwall serpentinite and overlying pillow basalts. The latter are covered by clastic materials which include abundant ultramafic–mafic detritus (Zakharov and Zakharova, 1975; Seravkin et al., 2001). According to recent biostratigraphic dating of conglomeratic interlayers, the basaltic and clastic units are of post-Silurian, possibly Early–Mid Devonian age (Seravkin et al., 2001).

The sulfide mineralization comprises massive, stockwork and disseminated ores consisting of pyrrhotite ± pyrite ± chalcopyrite assemblages, locally with chalcopyrite–cubanite intergrowths. Accessory minerals are chromite, cobaltite, sphalerite, Co-pyrite, Co-pentlandite, Ni-glaucodot as well as traces of native gold, native bismuth and pilsenite (Bi-telluride). Nickel is slightly enriched (0.2–0.4%) in ultramafic-hosted ores, whereas cobalt and copper are enriched (0.04–0.1% and 1.8%, respectively) in mafic-hosted ores (Zakharov and Zakharova, 1975). The uppermost ore level is characterized by network-like aggregates of lamellar pyrrhotite with interstitial Mg-rich saponite, chlorite, Fe-rich talc, quartz or dolomite (Nimis et al., in press). These aggregates are noteworthy for their strict resemblance to textures found in modern seafloor hydrothermal mounds at Middle Valley, Juan de Fuca Ridge, and Escanaba Trough, Gorda Ridge (cf. Goodfellow and Franklin, 1993; Zierenberg et al., 1993). The mound-like level is capped by a decimetric breccia layer made of clasts totally replaced by (Mg, Fe)-carbonates and green saponite, set in a matrix made of green, chromian saponite, chromite fragments and disseminated, low-T (Fe, Ni)-sulfides (Nimis et al., in press) (Fig. 4f). The carbonatized clasts show ghosts that resemble the mesh textures typical of serpentinites. Sometimes they include millimetric, amoeboid chromite grains. The absence of clasts of the underlying ores and of clear tectonic microstructures suggests the sedimentary nature of this breccia.

2.2. Ishkinino

The Ishkinino sulfide deposit is situated 20 km west of the town of Gay (Fig. 1). It is located within an antiform structure (Fig. 2b), which involves three tectonic slices mainly composed of (upwards): (i) tholeiitic basalts and cherts, with carbonaceous schists and lenses of limestones, of Upper Silurian to possibly Early Devonian age (Sakmara strata; >300 m in thickness); (ii) a mélange of serpentinites after harzburgites and dunites (200–300 m), which occasionally include centimetric pockets and lenses of chromitite; (iii) basalts and basaltic andesites with calcalkaline to boninitic affinity (Simonov et al., 2002) and basaltic breccias (>500 m), gradually passing upwards to cherts, siltstones, sandstones and Middle Devonian olistostromes with olistolites of siltstones, cherts and basalts (>200 m) (Maslov et al., 1993; Zaykov et al., 2000a, 2002). Two ore zones, named Eastern and Western, respectively, occur at the edges of the antiform and are accompanied by talc and talc-carbonate hydrothermal alteration of serpentinites. The three main tectonic slices are overlain by a fourth slice made of cherts and terrigenous sediments of Late Devonian–Early Carboniferous age.

A pyrrhotite–pyrite–cobaltite–chalcopyrite–arsenopyrite mineralization with accessory chromite occurs within the serpentinite mélange sheet and composes seven ore bodies up to 15 m thick and several tens of meters long. Cobaltite mostly occurs at the peripheries of the bodies, where it can reach 60% of the ore. Three main ore types can be recognized based on material extracted from a prospecting shaft in the Eastern ore zone (Wipfler et al., 1999): (i) pyrite–pyrrhotite with massive, porphyry, and clastic textures with clasts of lath-like pyrrhotite aggregates and dissemination, veins and cement of pyrite, magnetite and calcite; (ii) chalcopyrite–pyrite–pyrrhotite with chalcopyrite veins and nests with arsenopyrite, pentlandite and violarite inclusions; (iii) chalcopyrite–arsenopyrite with banded texture, with rare pentlandite, violarite and Ni–Co–Fe sulfide. The nature of the Ishkinino ores is interpreted to reflect an original deposition of VHMS sulfides, followed by metamorphic annealing and, possibly, further epithermal overprint (Wipfler et al., 1999).

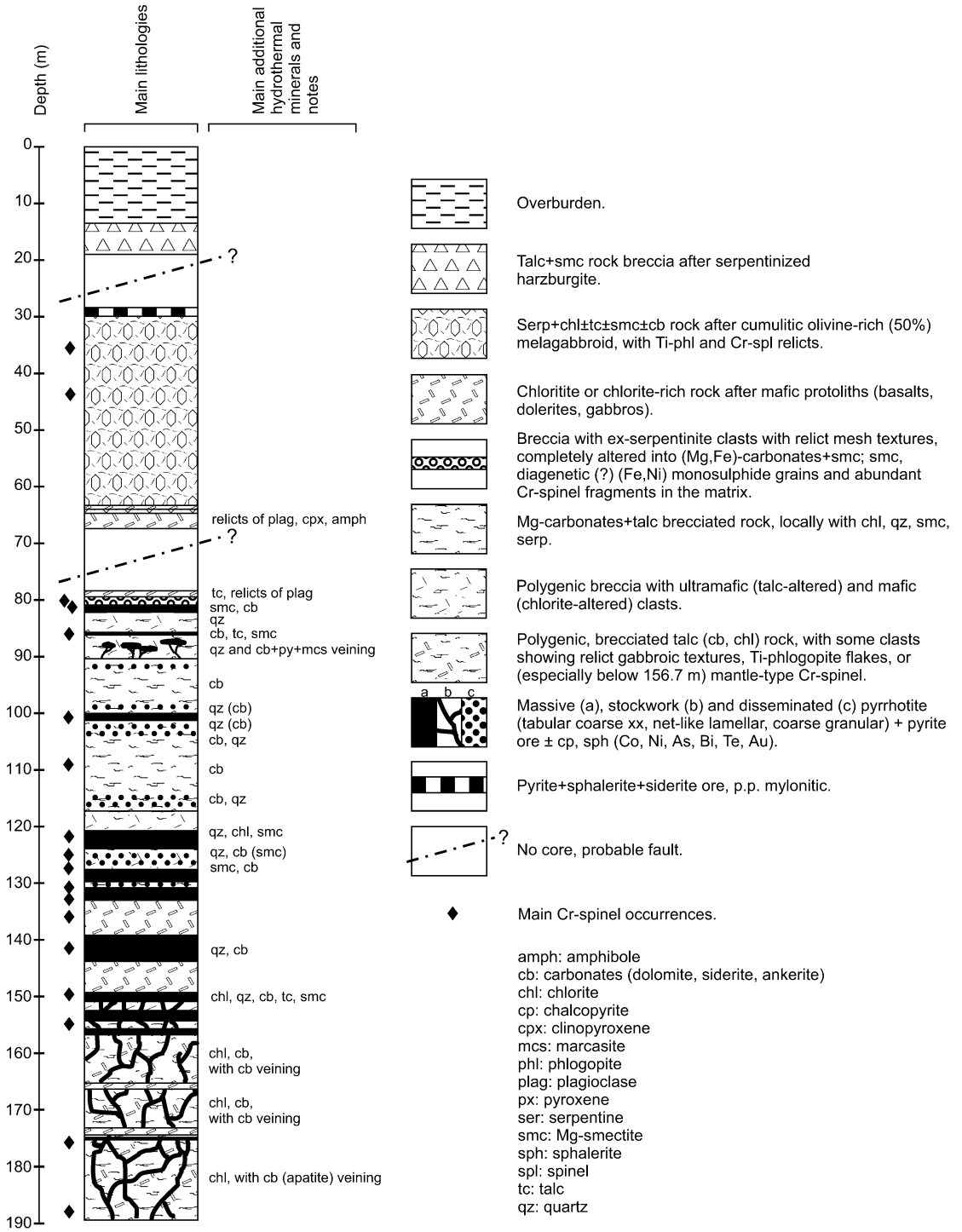

Fig. 3. Description of drillhole DDH2T, Ivanovka (cf. Fig. 2a).

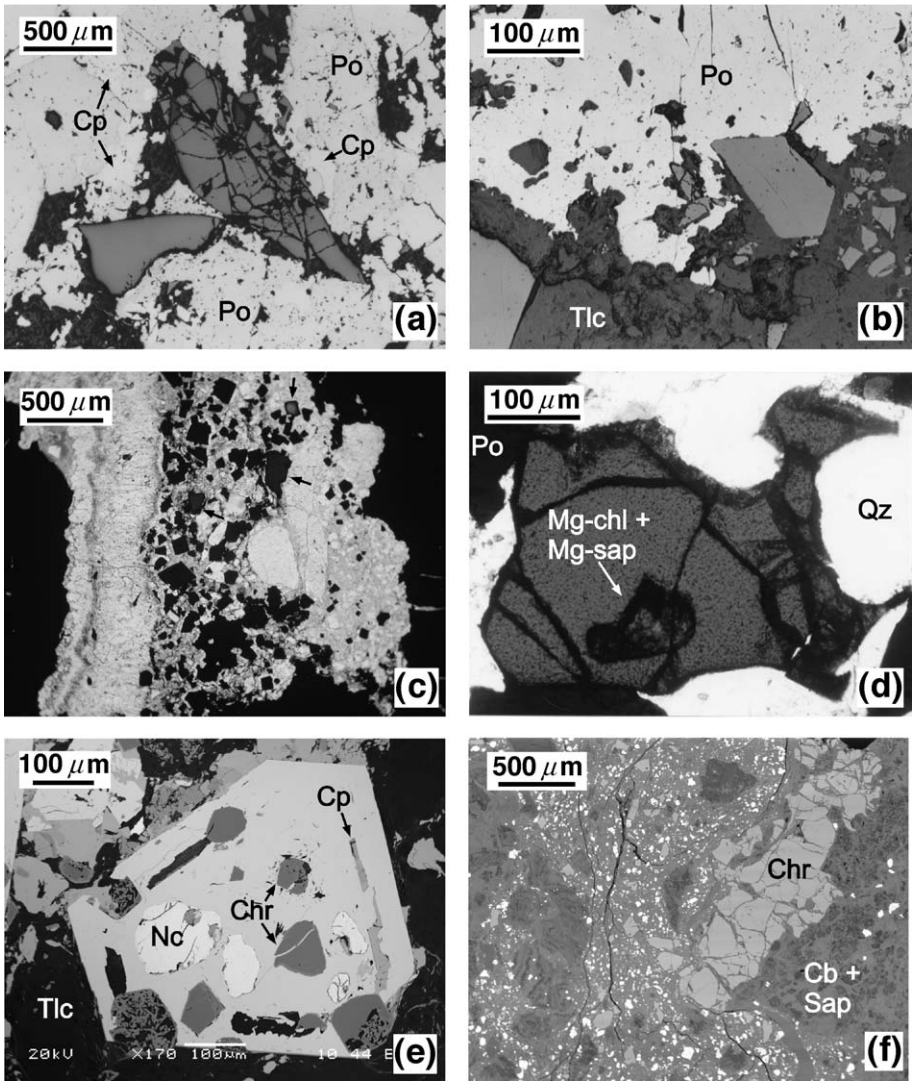

Fig. 4. Microphotographs of chromites from Ivanovka (#Iv) and Ishkinino (#Ish). (a) Cluster of chromite broken crystals (medium gray) associated with talc (dark gray; Tlc) interstitial to pyrrhotite (light gray; Po) + chalcopyrite (white; Cp) ore (#Iv155.4; reflected light). (b) Euhedral and fragmented chromite crystals in talc (dark gray) matrix and partly included in pyrrhotite (light gray; Po) (#Iv140.8; reflected light). (c) Fracture in massive pyrrhotite ore (black) filled by, from right to left: (i) a microbreccia of light gray fragments of chloritite in a Mg-saponite ± dolomite matrix with abundant idiomorphic cobaltite crystals (black) and a few nearly opaque euhedral crystals and fragments of chromite (arrows) and (ii) later veinlet of comb-like dolomite (#Iv132.7; plane-polarized transmitted light). (d) Irregular fragment of chromite crystal associated with quartz (Qz) as matrix of pyrrhotite ore (Po). The spinel carries an inclusion composed of Mg-chlorite + Mg-saponite (#Iv149.2; plane-polarized transmitted light). (e) Euhedral and fragmented chromite crystals (dark gray; Chr), with partially resorbed nickeline (white; Nc) and chalcopyrite (medium gray; Cp), included in late cobaltite crystal (light gray). Black matrix is talc. Spinels near the margin appear extensively transformed into porous ‘‘ferritchromit’’ (#Ish610-12; BSE image). (f) Breccia made of serpentinite clasts, transformed into carbonate (Cb; dark gray) + saponite (Sap; light gray), and chromite crystal fragments (medium gray) in a saponite matrix, capping the massive sulfide deposit. The big clast to the right includes an amoeboid chromite crystal (Chr). White, fine, disseminated crystals are of (Fe, Ni)-sulfides (#Iv80.3; BSE image).

3. Analytical methods and sample materials

Sample materials from the Ivanovka deposit were taken from a drillhole (DDH2T) obtained during a 1998 drilling campaign (Fig. 3). The drillhole is representative of the shallowest portions of the ore body and crosscuts several mineralized and barren levels. Sample materials from the Ishkinino deposit were taken from the damp of a prospecting shaft that crosscut the shallowest portion of the deposit (Fig.

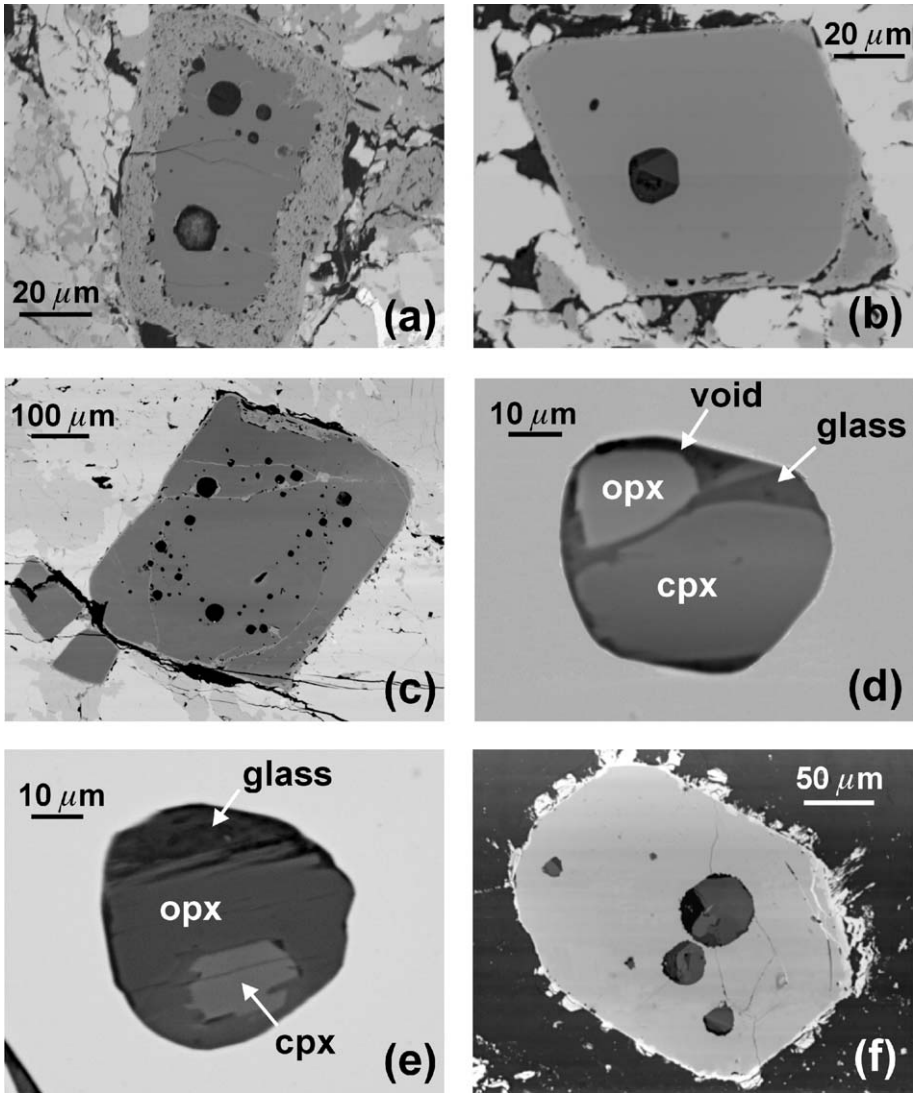

Fig. 5. BSE images of melt inclusions in chromites from Ivanovka (#Iv) and Ishkinino (#Ish). (a) Rounded and negative crystal melt inclusions with daughter pyroxenes in pyrrhotite + chalcopyrite matrix. The large inclusion near the bottom has been almost completely emptied during polishing. The host spinel shows a "ferritchromit" alteration rim and inclusions near the margins have been altered into Mg-chlorite (#Ish598-16). (b) Melt inclusion showing negative crystal shape, with faceted subcalcic-augite daughter crystal, in euhedral spinel crystal. The host spinel shows a tiny "ferritchromit" alteration rim (#Ish598-15). (c) Subhedral chromite in chalcopyrite–pyrite ore with melt inclusions along growth zone (#IshX). (d) Multiphase inclusion with void in the upper part. The light band between the glass and the hole is an artifact of sample topography (#Iv175.8). (e) Multiphase inclusion with cpx–opx intergrowth (#Iv175.8). (f) Euhedral spinel with glass (black) + pyroxenes (grey) + chalcopyrite (not visible) inclusions in serpentinite after harzburgite (#Ish1).

2b) and from surrounding outcrops. Polished thin sections of representative rocks, including both mineralized and barren types, were prepared for optical and scanning electron microscopy and for electron microprobe analysis. Chemical analyses of chromites and melt inclusions were carried out using a CAMECA "CAMEBAX" electron microprobe (CNR-IGG Padova) equipped with four vertical WDS spectrometers, operating at an accelerating voltage of 15 kV, beam current of 15 nA, counting time of 10 s for peak and 10 s for background, using a 1-μm beam. Natural and synthetic minerals (wollastonite for Ca and Si, albite for Na, orthoclase for K, vanadinite for V, sphalerite for Zn), pure oxides (for Al, Cr, Fe, MnTi and Ni) and elemental Co were used as standards. The CAMECA-PAP program was used

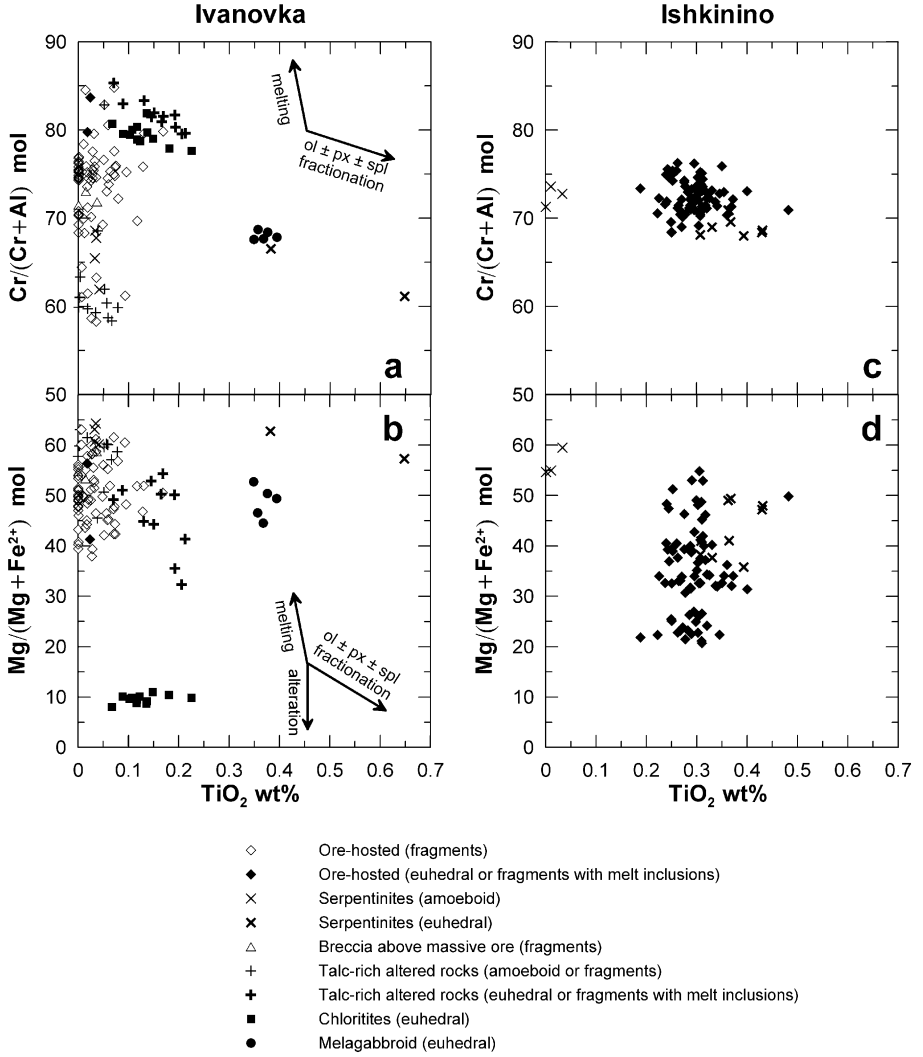

Fig. 6. Cr/(Cr + Al) vs. TiO_2 and Mg/(Mg + Fe^{2+}) vs. TiO_2 relations in chromites from Ivanovka (a, b) and Ishkinino (c, d). Solid and thick symbols are used for chromites of clear magmatic origin that occur as euhedral crystals or fragments carrying melt inclusions. Open and thin symbols are used for chromites that occur as non-euhedral amoeboid crystals or as fragments of uncertain origin. Approximate trends for peridotite partial melting, olivine ± pyroxene ± chromite fractionation and low-grade alteration are shown as arrows.

to convert X-ray counts into weight percent oxides. Analyses are believed to be precise to within ± 1–2% relative for major and ± 2–5% relative for minor oxides.

Scanning electron microscope (SEM) analyses were carried out using a CamScan MX2500 microscope, equipped with a tungsten cathode and four quadrant solid-state BSE detectors. Qualitative chemical microanalysis were carried out using an EDAX system with a "Sapphire" detector (LEAP + Si(Li) crystal). The analytical conditions were: 20 or 25 kV accelerating voltage, ~ 160 μA filament emission and 35 mm working distance.

4. Chromite in Ivanovka and Ishkinino ore fields

Chromite is a common accessory mineral in Ivanovka and Ishkinino sulfide ores, where it can represent up to 3% of the total, and in associated hydrothermally altered rocks. Ore-associated chromites occur either as disrupted grains (up to millimetric), which often form clusters of broken fragments, or as euhedral and subhedral octahedral crystals (up to 300 μm in size) (Figs. 4 and 5). Chromite fragments and octahedra are found either as inclusions in the sulfides (mostly pyrrhotite) or, more common, scattered in their talc ± chlorite ± saponite ± carbonate ± quartz matrix and veins (Fig. 4a, b, c, d). The chromites included in the sulfides tend to be located near the sulfide crystal margins (Fig. 4b). In the Ishkinino deposit, euhedral chromite is often included in cobaltite and arsenopyrite crystals (Fig. 4e). In both deposits, sulfide inclusions in chromite are rare. They are often located near the altered chromite rims or along partially healed cracks and usually have the same composition and optical orientation as the host sulfide. Multiphase history at Ivanovka is demonstrated by the presence of clasts made of chromite crystal fragments cemented by pyrite, which have been in turn cemented by later sulfides. Concentrations of chromite together with monazite crystals in a mixed sulfide–silicate breccia from the Ishkinino deposit are noteworthy.

Euhedral to subhedral chromite crystals similar to those associated with the sulfide ores occur in some serpentinized dunites–harzburgites from the Ishkinino ore field and in talc-rich rocks, in cumulate melagabbroids and, more rarely, in ore-associated chloritites and hanging wall pillow basalts from Ivanovka. Chromite in these rocks usually forms small (usually 5–10

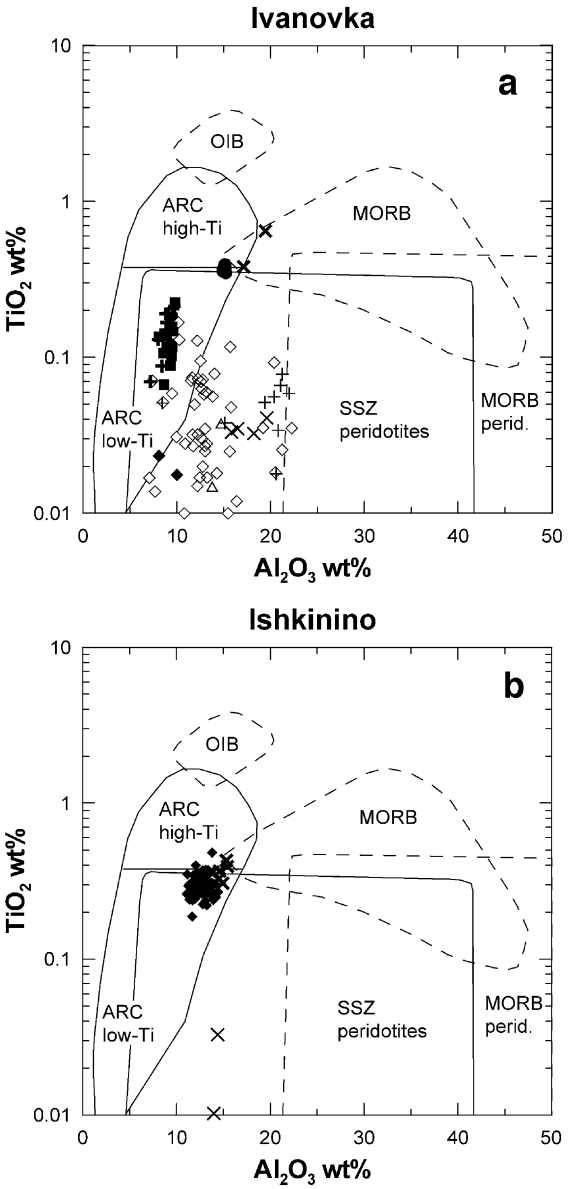

Fig. 7. TiO_2 vs. Al_2O_3 relations in chromites from Ivanovka (a) and Ishkinino (b). Fields for arc volcanic rocks, supra-subduction zone (SSZ) peridotites, ocean island basalts (OIB), and MORB basalts and peridotites after Kamenetsky et al. (2001). The *Arc low-Ti* field corresponds to boninitic and tholeiitic p.p. series; the *Arc high-Ti* field comprehends calcalkaline and tholeiitic p.p. series. Symbols as in Fig. 6. A few data with TiO_2 below 0.01 wt.% have been truncated.

μm and up to 1 mm) crystals, which are included in altered olivine and pyroxene crystals or scattered in interstitial position. In some serpentinites from both localities and in some talc-rich rocks from Ivanovka, chromite forms bigger grains (up to a few millimeters) which exhibit irregular to clearly amoeboid habits. Finally, at Ivanovka, high concentrations of detrital chromite (up to 3–5 modal %) occur in the breccia made of carbonatized serpentinite fragments that caps the main massive ore body (Fig. 4f).

Table 1
Representative electron microprobe analyses of chromian spinels from mafic–ultramafic rocks from Ivanovka and Ishkinino (all core analyses except where noted)

Rock	Basalt		Clastic[a]	Serpentinites					Olivine melagabbroid	
	1	2	3	4	5	6	7	8	9	10
Deposit	Ivanovka	Ivanovka	Ivanovka	Ivanovka	Ivanovka	Ishkinino	Ishkinino	Ishkinino	Ivanovka	Ivanovka
Sample	IvBz[b]	IvBz[b]	Iv80.3[c]	Iv3[b]	Iv10[b]	Ish8[b]	IS-0117[d]	Ish10-1b[b]	Iv44.0[c]	Iv36.0[c]
Habit	Euhedral (core)	Euhedral (rim)	Fragment	Amoeboid	Subhedral	Amoeboid	Subhedral	Subhedral	Euhedral	Euhedral
SiO_2	0.07	0.05	0.05	0.03	0.03	0.06	0.05	0.06	0.05	0.04
TiO_2	0.22	0.24	0.00	0.03	0.39	0.01	0.43	0.31	0.36	0.40
Al_2O_3	13.95	14.11	14.71	18.20	17.46	13.97	15.27	13.39	14.93	15.25
V_2O_3	n.a.	n.a.	n.a.	0.21	0.11	n.a.	n.a.	n.a.	0.15	0.13
Cr_2O_3	54.47	52.92	54.97	51.40	51.69	58.09	49.24	50.29	48.87	47.96
Fe_2O_3	3.55	3.64	1.93	1.90	1.98	0.12	5.26	5.38	5.10	6.42
FeO	13.63	18.16	16.56	13.87	14.13	16.67	19.32	21.14	19.29	18.57
MnO	0.28	0.31	0.39	0.24	0.35	0.29	0.43	0.36	0.29	0.26
MgO	13.32	10.47	11.25	13.34	13.38	11.42	9.70	8.23	9.43	10.18
CoO	n.a.	n.a.	n.a.	0.09	0.00	n.a.	n.a.	n.a.	0.00	0.00
NiO	0.07	0.01	0.05	0.06	0.05	0.11	0.09	0.08	0.13	0.08
ZnO	0.01	0.00	0.31	0.19	0.09	0.11	0.19	0.10	0.24	0.16
Total	99.58	99.91	100.20	99.57	99.67	100.85	99.98	99.33	98.83	99.45
Si	0.002	0.002	0.001	0.001	0.001	0.002	0.002	0.002	0.001	0.001
Ti	0.005	0.006	0.000	0.001	0.009	0.000	0.010	0.008	0.009	0.010
Al	0.525	0.539	0.556	0.672	0.646	0.526	0.584	0.525	0.579	0.584
V	0.000	0.000	0.000	0.005	0.003	0.000	0.000	0.000	0.004	0.004
Cr	1.375	1.357	1.394	1.274	1.284	1.467	1.263	1.322	1.271	1.233
Fe^{3+}	0.085	0.089	0.047	0.045	0.047	0.003	0.128	0.134	0.126	0.157
Fe^{2+}	0.364	0.493	0.444	0.364	0.371	0.445	0.524	0.588	0.531	0.505
Mn	0.008	0.009	0.010	0.006	0.009	0.008	0.012	0.010	0.008	0.007
Mg	0.634	0.506	0.538	0.623	0.626	0.544	0.469	0.408	0.462	0.493
Co	0.000	0.000	0.000	0.002	0.000	0.000	0.000	0.000	0.000	0.000
Ni	0.002	0.000	0.001	0.002	0.001	0.003	0.002	0.002	0.003	0.002
Zn	0.000	0.000	0.007	0.004	0.002	0.003	0.005	0.002	0.006	0.004
Sum	3.000	3.000	3.000	3.000	3.000	3.000	3.000	3.000	3.000	3.000
100Cr/(Cr+Al)	72.4	71.6	71.5	65.5	66.5	73.6	68.4	71.6	68.7	67.8
100Mg/(Mg+Fe^{2+})	63.5	50.7	54.8	63.1	62.8	55.0	47.2	41.0	46.6	49.4
Fe^{3+}/Fe^{2+}	0.23	0.18	0.10	0.12	0.13	0.01	0.24	0.23	0.24	0.31
Fe^{3+}/(Fe^{3+}+Ti+Cr+Al)	0.043	0.045	0.023	0.022	0.024	0.001	0.065	0.068	0.064	0.079

Unit formula and Fe^{3+} based on four oxygens and three cations.
w/incl.: with melt inclusions.
[a] Sedimentary breccia capping massive sulphide body.
[b] Samples taken from outcrops.
[c] Samples taken from drillhole DDH2T (numbers indicate depth in meters).
[d] Sample taken from shaft damp.

5. Chromite chemistry

The compositions of the cores of chromites from sulfide ores and mafic–ultramafic host rocks are illustrated in Figs. 6 and 7. Representative analyses are reported in Tables 1 and 2. The compositions range from magnesiochromite to chromite sensu stricto. Some crystals exhibit a highly reflectant, porous, iron-rich alteration rim having a composition corresponding to "ferritchromit" (cf. Burkhard, 1993)

Talc ± carbonate ± chlorite ± quartz ± saponite ± serpentine rocks								Chloritites	
11	12	13	14	15	16	17	18	19	20
Ivanovka	Ivanovka	Ivanovka	Ivanovka	Ivanovka	Ivanovka	Ivanovka	Ivanovka	Ivanovka	Ivanovka
Iv108.4[c]	Iv108.4[c]	Iv14.0[c]	Iv14.0[c]	Iv14.0[c]	Iv14.0[c]	Iv14.0[c]	Iv155.4[c]	Iv134.9[c]	Iv135.5[c]
Fragment	Fragment	Fragment (w/incl.)	Fragment (w/incl.)	Fragment (w/incl.)	Fragment (w/incl.)	Euhedral	Euhedral	Euhedral	Euhedral
0.05	0.03	0.02	0.05	0.00	0.04	0.03	0.09	0.04	0.06
0.06	0.00	0.21	0.19	0.21	0.15	0.19	0.07	0.13	0.15
21.95	20.71	9.59	9.13	9.73	8.81	8.78	7.17	9.71	9.79
0.16	0.13	0.24	0.19	0.22	0.24	0.22	0.20	0.08	0.13
46.56	48.33	55.61	55.54	56.78	59.67	58.58	62.20	53.61	54.93
1.63	2.03	4.80	4.42	4.07	1.70	5.07	1.56	3.31	1.83
15.11	15.29	23.41	22.23	20.79	19.57	18.00	17.86	29.82	29.43
0.28	0.17	0.55	0.38	0.32	0.27	0.32	0.33	0.55	0.50
12.78	12.81	6.28	6.88	8.23	8.75	10.18	9.70	1.88	2.04
0.00	0.00	0.17	0.09	0.03	0.02	0.07	0.06	0.00	0.05
0.11	0.08	0.01	0.10	0.09	0.00	0.03	0.03	0.01	0.10
0.27	0.12	0.44	0.18	0.13	0.23	0.15	0.03	0.36	0.50
98.96	99.70	101.34	99.37	100.61	99.46	101.62	99.29	99.50	99.50
0.001	0.001	0.001	0.002	0.000	0.001	0.001	0.003	0.002	0.002
0.001	0.000	0.005	0.005	0.005	0.004	0.005	0.002	0.003	0.004
0.806	0.759	0.380	0.368	0.383	0.350	0.339	0.285	0.404	0.406
0.004	0.003	0.006	0.005	0.006	0.006	0.006	0.005	0.002	0.004
1.146	1.188	1.480	1.500	1.498	1.590	1.518	1.660	1.496	1.530
0.038	0.047	0.122	0.114	0.102	0.043	0.125	0.040	0.088	0.049
0.394	0.398	0.659	0.635	0.580	0.552	0.494	0.504	0.880	0.867
0.007	0.004	0.016	0.011	0.009	0.008	0.009	0.009	0.016	0.015
0.593	0.594	0.315	0.351	0.409	0.439	0.497	0.488	0.099	0.107
0.000	0.000	0.005	0.002	0.001	0.001	0.000	0.002	0.000	0.001
0.003	0.002	0.000	0.003	0.002	0.000	0.001	0.001	0.000	0.003
0.006	0.003	0.011	0.005	0.003	0.006	0.004	0.001	0.009	0.013
3.000	3.000	3.000	3.000	3.000	3.000	3.000	3.000	3.000	3.000
58.7	61.0	79.6	80.3	79.7	82.0	81.7	85.3	78.7	79.0
60.1	59.9	32.4	35.6	41.4	44.3	50.2	49.2	10.1	11.0
0.10	0.12	0.18	0.18	0.18	0.08	0.25	0.08	0.10	0.06
0.019	0.024	0.061	0.057	0.051	0.022	0.063	0.020	0.044	0.024

Table 2
Representative electron microprobe analyses of ore-associated chromian spinels from the Ivanovka (drillhole DDH2T; sample numbers indicate depth in meters) and Ishkinino (shaft damp) deposits (all core analyses except where noted)

	1	2	3	4	5	6	7	8	9	10	11	12	13	14	15	16	17
Deposit	Ivanovka	Ivanovka	Ivanovka	Ivanovka	Ivanovka	Ivanovka	Ivanovka	Ivanovka	Ivanovka	Ivanovka	Ishkinino	Ishkinino	Ishkinino	Ishkinino	Ishkinino	Ishkinino	Ishkinino
Sample	Iv82.25	Iv86.9	Iv86.9	Iv100.1	Iv121.45	Iv122.4	Iv126.8	Iv126.8	Iv149.2	Iv175.8	Ish610-11	Ish610-11	Ish610-11	Ish610-12A	Ish598-15	Ish598-15	Ish598-15
Host	Matrix	Matrix	Matrix	Py	Matrix	Matrix	Matrix	Po	Matrix	Matrix	Po	Po	Apy	Po	Po	Po	Po
Habit	Fragment (w/ol)	Fragment (core)	Fragment (rim)	Fragment	Fragment	Fragment	Subhedral (w/incl.)	Fragment	Fragment	Fragment (w/incl.)	Subhedral	Euhedral (w/incl.)	Euhedral	Euhedral	Euhedral	Euhedral	Euhedral (w/incl.)
SiO_2	0.04	0.04	0.03	0.03	0.02	0.01	0.03	0.03	0.04	0.03	0.04	0.02	0.03	0.00	0.04	0.06	0.04
TiO_2	0.00	0.03	0.00	0.01	0.08	0.04	0.02	0.01	0.03	0.02	0.31	0.25	0.27	0.31	0.24	0.32	0.29
Al_2O_3	14.80	13.00	12.32	19.03	14.01	22.25	8.08	7.67	12.71	10.01	12.83	13.97	14.40	13.36	11.68	12.95	12.88
V_2O_3	0.16	0.25	0.19	0.16	0.22	0.08	0.15	0.10	0.14	0.22	0.23	0.23	0.28	0.24	0.20	0.22	0.25
Cr_2O_3	52.34	57.02	53.84	51.36	54.30	46.32	61.75	62.50	58.18	58.87	47.59	47.57	47.80	49.12	52.13	52.30	52.75
Fe_2O_3	2.45	0.14	2.31	1.37	3.14	2.71	0.63	0.93	0.41	2.17	6.44	6.17	5.87	6.74	6.17	4.75	4.88
FeO	18.76	19.26	21.08	14.01	15.86	14.92	20.29	19.67	16.18	16.00	27.31	26.14	23.04	21.33	21.17	19.47	17.17
MnO	0.30	0.34	0.36	0.25	0.20	0.21	0.45	0.43	0.34	0.33	0.30	0.22	0.22	0.40	0.31	0.31	0.23
MgO	9.61	9.38	7.68	13.45	11.73	13.20	8.02	8.54	11.35	11.28	4.00	5.01	6.63	7.98	8.10	9.37	10.87
CoO	0.00	0.00	0.00	0.00	0.00	0.00	0.00	0.00	0.00	0.00	0.17	0.14	0.56	0.12	0.13	0.09	0.09
NiO	0.03	0.01	0.06	0.06	0.12	0.10	0.00	0.00	0.00	0.03	0.05	0.08	0.20	0.16	0.10	0.07	0.02
ZnO	0.24	0.13	0.17	0.18	0.17	0.19	0.36	0.22	0.11	0.17	0.26	0.24	0.29	0.16	0.15	0.19	0.07
Total	98.73	99.62	98.03	99.89	99.86	100.02	99.78	100.10	99.49	98.96	99.52	100.05	99.60	99.91	100.42	100.09	99.54
Si	0.001	0.001	0.001	0.001	0.001	0.000	0.001	0.001	0.001	0.001	0.001	0.001	0.001	0.000	0.001	0.002	0.001
Ti	0.000	0.001	0.000	0.000	0.002	0.001	0.001	0.000	0.001	0.000	0.008	0.006	0.007	0.008	0.006	0.008	0.007
Al	0.573	0.504	0.492	0.698	0.531	0.807	0.323	0.305	0.487	0.390	0.518	0.555	0.567	0.522	0.457	0.501	0.496
V	0.004	0.007	0.005	0.004	0.006	0.002	0.004	0.003	0.004	0.006	0.006	0.006	0.008	0.006	0.005	0.006	0.007
Cr	1.360	1.482	1.442	1.264	1.382	1.126	1.654	1.666	1.495	1.540	1.291	1.268	1.262	1.288	1.369	1.357	1.361
Fe^{3+}	0.060	0.003	0.059	0.032	0.076	0.063	0.016	0.024	0.010	0.054	0.166	0.157	0.147	0.168	0.154	0.117	0.120
Fe^{2+}	0.515	0.530	0.597	0.365	0.427	0.384	0.575	0.555	0.440	0.444	0.783	0.737	0.644	0.591	0.588	0.534	0.469
Mn	0.008	0.009	0.010	0.007	0.006	0.005	0.013	0.012	0.009	0.009	0.009	0.006	0.006	0.011	0.009	0.009	0.006
Mg	0.471	0.460	0.388	0.624	0.563	0.605	0.405	0.429	0.550	0.556	0.205	0.252	0.330	0.394	0.401	0.458	0.529
Co	0.000	0.000	0.000	0.000	0.000	0.000	0.000	0.000	0.000	0.000	0.005	0.004	0.015	0.003	0.003	0.002	0.002
Ni	0.001	0.000	0.002	0.002	0.003	0.002	0.000	0.000	0.000	0.001	0.001	0.002	0.005	0.004	0.003	0.002	0.001
Zn	0.006	0.003	0.004	0.004	0.004	0.004	0.009	0.006	0.003	0.004	0.007	0.006	0.007	0.004	0.004	0.005	0.002
Sum	3.000	3.000	3.000	3.000	3.000	3.000	3.000	3.000	3.000	3.000	3.000	3.000	3.000	3.000	3.000	3.000	3.000
100Cr/(Cr + Al)	70.4	74.6	74.6	64.4	72.2	58.3	83.7	84.5	75.4	80.6	71.3	69.6	69.0	71.2	75.0	73.0	73.3
100Mg/(Mg + Fe^{2+})	47.7	46.5	39.4	63.1	56.9	61.2	41.3	43.6	55.6	55.3	20.7	25.5	33.9	40.0	40.6	46.2	53.0
Fe^{3+}/Fe^{2+}	0.12	0.01	0.10	0.09	0.18	0.16	0.03	0.04	0.02	0.12	0.21	0.21	0.23	0.28	0.26	0.22	0.26
$Fe^{3+}/(Fe^{3+} + Ti + Cr + Al)$	0.030	0.002	0.030	0.016	0.038	0.031	0.008	0.012	0.005	0.027	0.084	0.079	0.074	0.085	0.078	0.059	0.060

Unit formula and Fe^{3+} based on four oxygens and three cations.

w/ol: with olivine inclusion; w/incl.: with melt inclusions; matrix: part of matrix of sulphide ore; Po, Py, Apy: included in pyrrhotite, pyrite or arsenopyrite crystals.

(Fig. 5a, b, c; Table 3). This type of alteration is overwhelmingly more developed in the Ishkinino ores, where small euhedral crystals can be totally transformed into "ferritchromit". A chromian magnetite may also develop either as overgrowths or as further alteration products on the "ferritchromit" rim. The "ferritchromit" rims, where present, show abrupt contacts with the inner portions of the grains. The latter remain mostly unzoned, except a slight rimward decrease in $Mg/(Mg+Fe^{2+})$ ratios (see analyses 2 and 3 in Table 2). Moreover, their SiO_2 contents are invariably low (<0.3 wt.%) and unrelated to the contents of other major oxides. All these observations indicate that the composition of the cores of the chromite crystals were not significantly modified by low-grade alteration processes, except some degree of reequilibration of fast-diffusing divalent cations (cf. Barnes, 2000). This is also supported by the fact that

Table 3
Representative electron microprobe analyses of "ferritchromits" from the Ivanovka and Ishkinino ore fields

	1	2	3	4	5	6
Deposit	Ivanovka	Ivanovka	Ivanovka	Ishkinino	Ishkinino	Ishkinino
Sample no.	Iv108.4[a]	Iv10[b]	Iv14.0[c]	Ish610-12A[c]	Ish598-15[c]	Ish598-15[c]
Matrix	Talc rock	Serpentinite	Talc rock	Po ore	Po ore	Po ore
Habit	Fragment	Fragment (rim)	Fragment	Euhedral (rim)	Euhedral (rim)	Euhedral (rim)
SiO_2	0.07	0.06	0.08	0.03	0.09	0.07
TiO_2	0.97	0.92	0.19	0.72	1.18	0.28
Al_2O_3	1.85	3.14	0.38	1.06	0.80	1.26
V_2O_3	0.42	0.17	0.14	0.57	0.55	0.13
Cr_2O_3	40.94	41.01	22.44	54.77	43.92	17.79
Fe_2O_3	22.65	21.20	43.36	9.92	20.57	49.11
FeO	30.04	27.46	29.22	30.95	30.96	30.93
MnO	0.32	0.94	0.66	0.50	0.29	0.25
MgO	1.17	2.46	0.38	0.52	0.84	0.37
CoO	0.00	0.00	0.07	0.06	0.10	0.04
NiO	0.00	0.03	0.35	0.08	0.03	0.04
ZnO	0.16	0.23	0.00	0.24	0.36	0.22
Total	98.96	97.61	97.27	99.42	99.68	100.48
Si	0.003	0.002	0.003	0.001	0.004	0.002
Ti	0.027	0.026	0.006	0.020	0.033	0.008
Al	0.082	0.138	0.017	0.047	0.035	0.056
V	0.012	0.005	0.004	0.017	0.016	0.004
Cr	1.209	1.207	0.691	1.615	1.297	0.529
Fe^{3+}	0.637	0.594	1.270	0.279	0.578	1.390
Fe^{2+}	0.950	0.855	0.951	0.966	0.967	0.973
Mn	0.010	0.030	0.022	0.016	0.009	0.008
Mg	0.065	0.136	0.022	0.029	0.047	0.021
Co	0.000	0.000	0.002	0.002	0.003	0.001
Ni	0.000	0.001	0.011	0.002	0.001	0.001
Zn	0.004	0.006	0.000	0.007	0.010	0.006
Sum	3.000	3.000	3.000	3.000	3.000	3.000
100Cr/(Cr+Al)	93.7	89.7	97.6	97.2	97.4	90.5
$100Mg/(Mg+Fe^{2+})$	6.4	13.8	2.3	2.9	4.6	2.1
Fe^{3+}/Fe^{2+}	0.67	0.69	1.34	0.29	0.60	1.43
$Fe^{3+}/(Fe^{3+}+Ti+Cr+Al)$	0.326	0.302	0.640	0.142	0.297	0.701

Unit formula and Fe^{3+} based on four oxygens and three cations.

[a] Sample taken from drillhole DDH2T (numbers indicate depth in meters).

[b] Sample taken from outcrops.

[c] Sample taken from shaft damp.

melt inclusions (see next section) are usually well preserved when occurring within the inner portion of the chromite host, while they may show alteration into hydrous hydrothermal silicates (talc, Mg-saponite, Mg-chlorite, serpentine) when occurring near the chromite margins (Fig. 5a). To minimize the effect of subsolidus reequilibration and hydrothermal alteration, only analyses of chromite cores that showed negligible or minor Mg → Fe zoning have been selected for the present work. However, given the small size of most chromite crystals, the absence of significant zoning may at least in part be the result of intracrystalline diffusion and rehomogenization. Therefore, the measured contents of divalent cations are not necessarily representative of the original chromite compositions.

Chromites from Ivanovka have 100Cr/(Cr + Al) atomic ratios (hereafter Cr#) ranging between 56 and 88, and 100Mg/(Mg + Fe^{2+}) atomic ratios (hereafter Mg#) ranging between 8 and 64 (Fig. 6a and b). They are characterized by highly variable Fe^{3+}/Fe^{2+} atomic ratios (0.00–0.35) and, except a few euhedral chromites from melagabbroids and serpentinites, by relatively low (≤ 0.23 wt.%) TiO_2 contents (Tables 1 and 2; Fig. 7a). Amoeboid chromites from serpentinites and detrital chromites in the breccia capping the main massive sulfide orebody show the lowest TiO_2 contents (< 0.05 wt.%). A group of Cr-rich (Cr# = 80–85) euhedral–subhedral chromites from talc-altered rocks shows a slight but definite increase in TiO_2 with decreasing Cr# and Mg# (Fig. 6a and b). In all other samples from Ivanovka, variations in Cr# and Mg# ratios do not appear to be associated with a systematic change in TiO_2 contents, although overlap of different populations of data may have obscured any existing correlation. Chromites from chloritites form a distinct group characterized by Mg# values about 10, only moderately high TiO_2 (0.06–0.23 wt.%), high ZnO contents (up to 0.8 wt.%), and Fe^{3+}/Fe^{2+} ratios close to 0.1. The contents of zinc and nickel in the other samples are variable, reaching ca. 0.4 wt.% ZnO in a few chromites in sulfides and talc-rich rocks and 0.6 wt.% NiO in other ore-hosted chromites. Vanadium contents are mostly between 0.1 and 0.3 wt.% V_2O_3, and reach 0.5 wt.% in some ore-hosted examples.

Chromites from Ishkinino ores form a coherent group characterized by decreasing Mg# (from 55 to 20) and little varied Cr# ratios and TiO_2 contents (Cr# = 68–76; TiO_2 = 0.2–0.5 wt.%) (Figs. 6c, d and 7b). The decrease of Mg# at virtually constant Cr# and TiO_2 is consistent with zoning patterns found in individual crystals. Fe^{3+}/Fe^{2+} atomic ratios are relatively high and vary within a restricted range (0.16–0.37). The contents of zinc, nickel and vanadium are comparable with those in the ore-hosted chromites from Ivanovka, with maximum contents of 0.4 wt.% ZnO, 0.4 wt.% NiO and 0.3 wt.% V_2O_3. Chromites included in cobaltite and arsenopyrite are slightly enriched in CoO (up to 0.6 wt.%). Compared with the ore-hosted chromites, euhedral and subhedral chromites from Ishkinino serpentinites have similar Mg# (36–49) and Fe^{3+}/Fe^{2+} ratios (0.19–0.26), and similar or slightly lower Cr# values (68–72). Amoeboid chromites from Ishkinino serpentinites have lower Mg# (55–60), comparable Cr# (71–74), and much lower Fe^{3+}/Fe^{2+} ratios (0.01–0.04).

Compared with the compositions of the chromite cores, the altered "ferritchromit" rims are enriched in $Fe_{tot.}$, Mn and Ti, are strongly depleted in Al and Mg and have higher relative proportion of oxidized vs. reduced iron, corresponding to higher contents of magnetite and chromite components (Table 3). Some are also enriched in V_2O_3 (up to 0.6 wt.%) and ZnO (up to 0.5 wt.%).

6. Melt and mineral inclusions in chromites

Euhedral and subhedral chromites from both sulfide ores and associated rocks frequently carry multiphase inclusions of glass and/or anhydrous silicate minerals up to 40 μm in size (Fig. 5). The inclusions show either round or negative crystal forms. They are usually randomly scattered within the host mineral (Fig. 5a and b); more rarely, they are aligned along crystal growth zones (Fig. 5c). Apart from tiny "ferritchromit" alterations (Fig. 5a, b, c) and slight rimward decrease in Mg# values (see Section 5), the host chromites appear homogenous and mostly free of fissures or cracks. Such features indicate that the inclusions are primary and contain partly crystallized liquids parental to the host chromites (cf. Roedder, 1984).

The inclusions generally contain an aggregate of daughter minerals, a small-volume residual glass and,

sometimes, voids which probably represent former liquid or gaseous bubbles (Fig. 5d and e). Representative analyses of glass and daughter minerals in melt inclusions are reported in Table 4. High-quality analyses were often difficult to obtain owing to the small size of the inclusions and to the presence of voids. Silicate daughter minerals comprise irregular, round or rarely euhedral crystals of enstatitic orthopyroxene and diopsidic to subcalcic, augitic clinopyroxenes (Fig. 5d and e). Intergrowths of diopside with enstatite or subcalcic augite are common. The subcalcic augites have Al_2O_3, FeO and, sometimes, Na_2O contents higher than in the other pyroxenes. These features are typical of quench subcalcic clinopyroxenes formed under nonequilibrium conditions in subalkaline basalts (e.g. Smith and Lindsley, 1971).

The residual glasses are characterized by high SiO_2 (63–76 wt.% recalculated on anhydrous basis from a set of four analyses from Ivanovka and seven analyses from Ishkinino), variable Al_2O_3 (9–19 wt.%), MgO (0–20 wt.%) and Na_2O (4–10 wt.%), low CaO (0–6 wt.%) and FeO (0.2–2.2 wt.%), very low K_2O ($\leq$0.06 wt.%, with one exception at 0.67 wt.%) and TiO_2 ($\leq$0.05 wt.%, with one exception at 0.18 wt.%) and usually significant Cr_2O_3 ($\leq$1.5 wt.%) contents. Occasionally, micron-sized (Fe, Cu, Ni)-sulfide blebs occur in the glass. The occurrence of sulfide blebs and former gaseous or liquid bubbles suggests that the original inclusions consisted of either a homogenous (H_2O + S)-bearing silicate melt or a supercritical silica-rich fluid (Schiano et al., 1995). In the absence of rehomogenization data, the low residual melt/daughter

Table 4
Representative electron microprobe analyses of glass and daughter minerals (analyses 1–4) and of isolated mineral inclusions (analyses 5–7) in ore-associated chromian spinels from Ivanovka (drillhole DDH2T; sample numbers indicate depth in meters) and Ishkinino (shaft damp) deposits (cf. analyses 1, 10 and 12 in Table 2)

Sample	Iv175.8			Ish610-11	Iv82.25		Iv175.8
	1	2	3	4	5	6	7
Phase	Glass	cpx	opx	Glass[a]	ol	opx	cpx
SiO_2	62.95	53.94	57.87	70.25	41.02	57.15	54.01
TiO_2	0.01	0.01	0.02	0.03	0.01	0.00	0.02
Al_2O_3	9.63	0.88	0.49	17.01	0.02	0.95	1.74
Cr_2O_3	0.91	2.00	1.23	1.10	0.93	0.96	1.80
FeO	0.63	1.74	4.79	0.73	7.34	5.65	1.79
MnO	0.00	0.05	0.14	0.05	0.13	0.13	0.00
MgO	20.16	17.60	35.96	0.64	51.26	34.87	20.10
CaO	0.43	23.54	0.51	0.05	0.01	1.28	19.07
Na_2O	4.12	0.53	0.02	10.08	0.01	0.00	1.00
K_2O	0.67	0.01	0.01	0.06	n.a.	0.02	0.00
NiO	n.a.	n.a.	n.a.	n.a.	0.34	n.a.	n.a.
Total	99.50	100.31	101.05	100.00	101.07	101.00	99.53
Si		1.958	1.968		0.990	1.956	1.951
Ti		0.000	0.001		0.000	0.000	0.001
Al		0.038	0.020		0.000	0.038	0.074
Cr		0.057	0.033		0.018[b]	0.026	0.051
Fe		0.053	0.136		0.148	0.162	0.054
Mn		0.002	0.004		0.003	0.004	0.000
Mg		0.952	1.823		1.844	1.779	1.082
Ca		0.915	0.018		0.000	0.047	0.738
Na		0.038	0.002		0.000	0.000	0.070
K		0.000	0.000		–	0.001	0.000
Ni		–	–		0.005	–	–
Sum		4.013	4.006		3.010	4.012	4.021

Unit formulas based on six oxygens for pyroxenes and four oxygens for olivine.
Labels: cpx, Ca-rich clinopyroxene; opx, orthopyroxene; ol, olivine; n.a.: not analyzed.
[a] Inclusion contained daughter orthopyroxene.
[b] Calculated as Cr^{2+}.

minerals volume ratios do not allow a quantitative estimate of the original compositions of the melts. However, the compositions of the residual glasses and the absence of daughter minerals other than pyroxenes suggest that the original melt compositions had SiO_2 greater than ca. 55 wt.% (mean composition of daughter pyroxenes) and K_2O lesser than ca. 0.7 wt.% (maximum measured value in the residual glasses).

Highly magnesian (Fo_{92-95}), Cr-rich ($Cr_2O_3 = 0.7–1.3$ wt.%) olivine, sometimes in association with chromian enstatite, and chromian diopside have also been rarely found as isolated, round or subround, melt-free inclusions (Table 4). The unusually high measured contents of chromium in olivine are possible at very high temperature or at very low oxygen fugacities, where the fraction of the reduced species Cr^{2+} becomes significant, and are also favored by high activities of silica in the melt and of $MgCr_2O_4$ component in the coexisting spinel (Lehman, 1983; Li et al., 1995). However, contamination of electron microprobe analyses by the host chromite may as well in part explain the measured Cr contents and may perhaps account for the apparent slight cation excess and Si deficiency of the analyses (Table 4).

7. Discussion

7.1. Chromite–sulfide textural relations

Melekestseva et al. (2001) reported pyrite + chalcopyrite inclusions in chromites as well as chromite inclusions in different sulfide minerals from Ishkinino. According to these authors, growth patterns expressed by Co and Ni zoning in cobaltite are cut by the chromite inclusions, whereas those in arsenopyrite surround the chromite inclusions. Melekestseva et al. (2001) interpreted these particular textural relations as reflecting a possible formation of chromite during deposition of the sulfide ores.

Other textural features, however, do not support a syngenetic relation between chromites and sulfides at Ivanovka and Ishkinino. First, sulfide inclusions in chromite are often located near the altered chromite rims or along partially healed cracks and usually have the same composition and optical orientation as the host sulfide. This implies that the sulfide inclusions may be secondary and that at least some of them may not be true inclusions but, rather, portions of late sulfides surrounding irregularly shaped chromite grains. Second, sulfide inclusions in chromite, whatever their nature, are rare, whereas the opposite relation is common. Third, chromite inclusions in sulfides often occur as broken fragments, clearly indicating that formation and disruption of the chromite crystals predated the deposition of the sulfides.

As for the relations between chromite inclusions and zoning patterns in cobaltite, we note that the interruption of zoning bands at the host–inclusion interface cannot be taken as an index of contemporaneous growth, unless the inclusion exhibits a negative crystal shape or the inclusion and the host show evidence of mutual growth interference (cf. Bulanova, 1995). In fact, the chromite inclusions in cobaltite described by Melekestseva et al. (2001) invariably exhibit their own euhedral habit (cf. Fig. 4e); therefore, a syngenetic relation between the inclusions and their hosts remains questionable.

Concentrations of euhedral chromite crystals in veins cutting earlier sulfides are problematic (Fig. 4c). In some cases, these veins are filled by a mixture of chromite crystals and fragments of host rocks (see chloritite clasts in Fig. 4c). This observation suggests that these chromites do not belong to late mineral parageneses but, rather, they were part of clastic materials that were introduced mechanically into discontinuities of fractured sulfide ores.

Although the mere textural relations between the chromites and the sulfides are not always unequivocal, we must conclude that there is no textural evidence that the formation of Ivanovka and Ishkinino chromites was contemporaneous to the deposition of the sulfides.

7.2. Morphological and compositional data

Indications about the origin of the studied chromites are provided by morphological and compositional data. Irregular, amoeboid chromites interstitial to olivine and pyroxene, such as those found in some of the studied serpentinites and talc-rich rocks, are typical of upper mantle peridotites that are believed to represent residues after partial melting (e.g. Dick, 1977). By contrast, euhedral chromites, such as those commonly found in some other studied serpentinites or in association with the Ivanovka and Ishkinino sulfide ores, are typical of cumulate mafic and ultra-

mafic rocks and podiform chromitites in ophiolitic sequences and are considered to reflect crystal growth from a free melt (e.g. Dick, 1977; Augé and Roberts, 1982; Augé, 1987). The presence of primary melt inclusions in many of these euhedral chromites unambiguously demonstrates their magmatic origin. Moreover, the occurrence of chromites with either euhedral or amoeboid shapes in several hydrothermally altered, talc-rich rocks from Ivanovka clearly indicates the heterogeneous nature of their protoliths. These must have included both mantle melting residues and mantle or crust cumulates.

In terms of chemical composition, chromian spinels in abyssal peridotites and MORB basalts related to the oceanic ridge system typically have Cr# <60 (cf. Type I of Dick and Bullen, 1984) and Al_2O_3 contents higher than ca. 20 wt.% (Fig. 7). In a compilation of 1265 analyses of spinels from MORB basalts by Barnes and Roeder (2001), Cr# values in the range 70–80 appear in less than 2% of the samples and no sample with Cr# >80 is reported. Cr# values greater than 60 (or Al_2O_3 <20 wt.%) imply high degrees of mantle melting and are typical of spinels from supra-subduction zone (SSZ) mantle peridotites and island arc or, less commonly, back-arc volcanic rocks (cf. Types II and III of Dick and Bullen, 1984) (Fig. 7). The above relations are not significantly modified by subsolidus reequilibration and low-grade alteration. These processes may induce an increase in Zn (Mn) contents and a decrease in Mg# values, while relative proportions of trivalent ions remain virtually unchanged up to low-amphibolite facies conditions (below ~ 500–550 °C; Barnes, 2000). Thus, discriminatory plots that use highly charged cations should be more robust to subsolidus reequilibration and alteration than those based on Mg and Fe contents (cf. Kamenetsky et al., 2001).

The compositions of amoeboid chromites from Ivanovka serpentinites and of detrital chromites in the breccia capping the main massive sulfide orebody strictly resemble those of chromites in SSZ mantle peridotites (Fig. 7a). More Al-rich (Al_2O_3 = 15–22 wt.%) chromites in some talc-rich rocks indicate lower degrees of mantle melting, but still within the field of typical SSZ peridotites (Fig. 7a).

The inverse correlations between TiO_2 contents and Mg# and Cr# numbers shown by high-Cr# (>80) magmatic chromites from other Ivanovka talc-rich rocks are consistent with crystallization from melts that underwent variable degrees of olivine ± pyroxene ± spinel fractionation (Fig. 6a and b). For these highly chromiferous spinels, the very high Cr# values and low TiO_2 contents (≤ 0.2 wt.%) suggest that the parent melts had an arc tholeiitic or boninitic affinity. In particular, the most iron-rich among these samples resemble some of the chromites from forearc high-Mg andesites (e.g. Bamus volcano, Papua New Guinea; Johnson et al., 1983). The approximate TiO_2 and Al_2O_3 contents of the melts parent to these chromites can be estimated from $(TiO_2)_{spinel}$ vs. $(TiO_2)_{melt}$ and $(Al_2O_3)_{spinel}$ vs. $(Al2O_3)_{melt}$ systematics in low-Al spinels (cf. Kamenetsky et al., 2001; their Fig. 4a and b). The estimated compositions have TiO_2 contents of less than ca. 0.3 wt.% and Al_2O_3 contents of 8–11 wt.%, respectively. These values, combined with the relatively high-SiO_2 (>55 wt.%) and low-K_2O (<0.7 wt.%) character of the melt inclusions (cf. Section 6), compare well with those of postulated boninitic primary magmas (e.g. Walker and Cameron, 1983).

Chromites from chloritites after mafic protoliths are particularly enriched in Fe^{2+}, although their Cr# values and TiO_2 contents remain comparable with those of the high-Cr# magmatic chromites in talc-rich rocks (Fig. 6a and b). In this group, the absence of any correlation between Mg# and TiO_2 suggests that low-grade alteration is at least in part responsible for the observed Fe enrichment. Euhedral chromites from olivine-rich melagabbroids and, especially, serpentinites are enriched in TiO_2 (up to 0.65 wt.%) compared to chromites in both talc-rich rocks and chloritites, suggesting derivation from more fractionated melts or an evolution towards higher-Ti tholeiitic or calcalkaline types (Fig. 7a).

The compositions of ore-hosted chromites from Ivanovka are scattered across the whole range of compositions of euhedral and amoeboid chromites in associated talc-rich and serpentinitic rocks and of detrital chromites in the hanging wall breccia (Figs. 6a, b and 7a). This observation suggests that the ore-hosted chromites have the same origin as those in the associated hydrothermally altered magmatic rocks and mantle melting residues.

The compositions of amoeboid chromites in Ishkinino serpentinites are well within the field of SSZ mantle peridotites (Fig. 7b). Euhedral and melt inclusion-bearing chromites from the Ishkinino ores show a

large scatter in Mg# values (Fig. 6d), which can primarily be ascribed to low-grade alteration. In the Cr# vs. TiO_2 and TiO_2 vs. Al_2O_3 plots, the compositions of these chromites are more uniform and displaced to slightly higher TiO_2 contents (0.19–0.48 wt.%) than those of most Ivanovka samples (Figs. 6c, d and 7b). The least chromiferous, most aluminiferous of these chromites approach in composition the euhedral chromites that occur in Ishkinino serpentinized harzburgites and dunites and in Ivanovka melagabbroids (Figs. 6c, d and 7b). The estimated compositions of the melts parent to Ishkinino chromites, calculated according to spinel–melt systematics (Kamenetsky et al., 2001), are characterized by low Al_2O_3 contents (8–12 wt.%), but are not so poor in TiO_2 (0.3–0.6 wt.%), indicating a stronger degree of magmatic fractionation or an evolution towards more tholeiitic or calcalkaline compositions compared with the majority of Ivanovka samples. The high and little varied Fe^{3+}/Fe^{2+} ratios indicate relatively uniform values of oxygen fugacity for all Ishkinino chromites of magmatic origin.

As for the significance of the oxidized, iron-enriched rims, we recall that "ferritchromit" is found both as an alteration product of chromites that forms during serpentinization and greenschist–amphibolite-facies metamorphism of ultramafic rocks (e.g. Burkhard, 1993; Barnes, 2000) and as a primary phase in association with magmatic Fe–Ni–Cu sulfide ores. The latter is characterized by distinctively high contents of Zn (>0.6 at.%; Groves et al., 1983), which do not exist in the "ferritchromits" studied here nor in any of the studied chromites. A magmatic origin for the "ferritchromits" can, therefore, be excluded. The development of the "ferritchromit" and magnetite rims in the studied chromites is ascribed to reactions with silicate minerals and oxidizing hydrous fluids during early oceanic alteration or during subsequent hydrothermal circulation and sulfide deposition.

7.3. Estimated crystallization temperatures

Pyroxene temperatures based on the graphic thermometer of Lindsley (1983) and compositions of coexisting clino- and orthopyroxene included in chromites from Ivanovka and Ishkinino (excluding subcalcic and highly aluminous "quench" compositions) are in the range 930–1170 °C at a nominal pressure of 1 GPa. Because of thermal relaxation during pyroxene crystallization and potential subsolidus reequilibration between the two pyroxenes, these values can be considered as minimum estimates for the temperatures of the melts at the time of entrapment and chromite crystallization. A single, apparently isolated clinopyroxene (Table 4, analysis 7), which was included in a millimetric chromite rich in melt inclusions and hosted in an ore-bearing talc–chlorite–carbonate rock from Ivanovka (Iv175.8), yielded a temperature of 1260 °C. The relatively low Na, Al and Fe contents suggest that this clinopyroxene is not a "quench" mineral. The absence of coexisting low-Ca pyroxene and the armor effect operated by the host chromite probably prevented this clinopyroxene from significant subsolidus reequilibration.

7.4. Geodynamic setting and mode of chromite and sulfide formation

Textural and compositional data on sulfide minerals as well as host-rock alteration sequences indicate that the Ivanovka and Ishkinino ore deposits formed by seafloor or subseafloor hydrothermal processes (Wipfler et al., 1999; Zaykov et al., 2000a; Nimis et al., in press). At Ishkinino, the original hydrothermal textures and parageneses have been partly modified by later remobilization, while at Ivanovka they have been almost entirely preserved. By contrast, compositional and morphological data and the presence of high-temperature melt inclusions in many crystals indicate that the ore-associated chromites consisted of a mixed population of spinels derived from mantle melting residues and cumulates of mantle and/or crustal origin. Cumulates potentially included both silicatic rocks and chromitites, and appear to have been dominant, if not exclusive, at Ishkinino. Given the contrasting origin of and the textural relationships between the sulfides and the chromites, we are forced to conclude that the chromites in the Ishkinino and Ivanovka deposits represent relicts derived from the ore-hosting rocks and have no genetic relationship with the associated ores.

Highly chromian, (Al, Ti)-poor spinels such as those studied here have never been found in abyssal peridotites and volcanics, which precludes a mid-ocean ridge origin for the studied mafic–ultramafic rocks of the MUFZ (e.g. Dick and Bullen, 1984; Kamenetsky et al., 2001; Barnes and Roeder, 2001).

The likely boninitic to low-Ti tholeiitic affinity of the melts parental to the studied spinels suggests formation in an early arc or forearc setting (e.g. Pearce et al., 1992; Bloomer et al., 1995). Consistently, the geochemistry of variously altered rocks from both Ivanovka and Ishkinino deposits, as well as the compositions of surrounding mafic volcanics and of melt inclusions found in some igneous pyroxenes, also point to a boninitic to island arc tholeiitic affinity (Simonov et al., 2002; and work in progress). In spite of the strong analogies between sulfide mineralogy in the studied deposits and in counterparts on modern oceanic spreading centers (e.g. Zaykov et al., 2000a), a mid-ocean ridge origin of the Ishkinino and Ivanovka deposits can, therefore, be excluded.

Tectonic activity within the arc–forearc system could favor exposure and brecciation of crust and mantle materials. This may account for the widespread occurrence of brecciated, sometimes polygenic, mafic–ultramafic lithologies (olistostromes? tectonic mélange?) and the frequent fragmented appearance of the chromite crystals in the studied ore-bearing sequences and in their surroundings. The locally high proportion of chromites suggests that the protoliths of the sulfide host-rocks may have included chromitites, such as those occurring occasionally in serpentinites from the Ishkinino area. High proportions of chromite in brecciated lithologies can also in part be explained by erosion of altered mantle and lower-crust rocks exposed on an uneven seafloor, followed by gravitative concentration during transport prior to sulfide mineralization. The occasional occurrence of chromite + monazite ''heavy-mineral'' concentrations at Ishkinino may also have a detrital origin, although a hydrothermal origin of monazite cannot be excluded.

Circulation of hydrothermal fluids through cracks and discontinuities of tectonic and/or sedimentary breccias could promote the deposition of disseminated to massive Fe–Cu–(Ni–Co) sulfide ores by metasomatic substitution. The refractory nature of the chromites led to their accumulation in the residual silicate-rich matrix and, in part, to their entrainment in the rim portions of the growing sulfide crystals. The occurrence of chromite crystals and chloritite fragments in Mg-saponite-carbonate matrix as filling of fractures in some ore samples (Fig. 4c) suggests that mechanical injection of altered and disrupted mafic–ultramafic materials through the sulfide ores, driven by circulation of pressured hydrothermal media, may locally have played a significant role. This process may also have led to selective concentration of high-density components such as chromite in preferential sites.

The presence of inclusions of relict chromite in the massive sulfides restrains the timing of sulfide deposition to after the formation of the chromite. The most probable time window for sulfide ore deposition is to be found between the onset of boninitic island arc magmatism in the Southern Urals, marked by volcanic rocks in the Baimak–Buribai region (ca. 400 Ma based on the new time scale of Tucker et al., 1998, and biostratigraphic data by Maslov et al., 1993) and the age of continent–arc collision, marked by high-pressure subduction metamorphism of the East European continental margin (Maksyutov Complex; 380–370 Ma; Scarrow et al., 2002; and references therein).

8. Conclusions

The main conclusions of the present work can be summarized as follows:

1. The chromites occurring in VHMS deposits of the southern MUFZ represent refractory relicts of hydrothermally altered and metasomatically replaced mafic–ultramafic rocks.
2. The chromite-bearing protoliths included mantle melting residues and mantle or crust cumulates that formed in a supra-subduction zone.
3. The chromite-bearing VHMS deposits did not form on a mid-ocean ridge but in an early-arc or forearc setting characterized by abundant brecciated serpentinites and island arc tholeiitic to, possibly, boninitic igneous rocks.

Acknowledgements

The authors are indebted to P. Omenetto (Padova) for his invaluable suggestions and comments, and to N. Tatarko (Bashkirgeologia, Ufa) for access to the Sibay lithotheque and Ivanovka drillhole. J.-J. Orgěval (BRGM, Orléans) is thanked for help during the 2001 Urals trip. I. Melekestseva (IMIN, Miass) is thanked for help in field work and her preliminary study of Cr-spinels from Ishkinino. R. Carampin and L. Peruzzo (CNR-IGG Padova) are thanked for

assistance during EMP and SEM analysis. Reviews by B. Oberger and V. Kamenetsky helped us significantly improve the manuscript. This work was carried out in the framework of the EU-funded MinUrals project INCO COPERNICUS ICA2 CT-2000-10011 (IMIN-Kroseven–BRGM Collaborative Partnership). P. Nimis gratefully acknowledges the financial support of the CNR-IGG (Padova) and Italian MURST ex 60% grants. S. Tesalina and V. Zaykov gratefully acknowledge the support of Russian Foundations RFFI no. 01-05-65329 and University of Russia.

References

Augé, T., 1987. Chromite deposits in the northern Oman ophiolite: mineralogical constraints. Miner. Depos. 22, 1–10.

Augé, T., Roberts, S., 1982. Petrology and geochemistry of some chromitiferous bodies within the Oman ophiolite. Ofioliti 7, 133–154.

Barnes, S.J., 2000. Chromite in komatiites: II. Modification during greenschist to mid-amphibolite facies metamorphism. J. Petrol. 41, 387–409.

Barnes, S.J., Roeder, P.L., 2001. The range of spinel compositions in terrestrial mafic and ultramafic rocks. J. Petrol. 42, 2279–2302.

Bloomer, S.H., Taylor, B., MacLeod, C.J., Stern, R.J., Fryer, P., Hawkins, J.W., Johnson, L., 1995. Early arc volcanism and the ophiolite problem: a perspective from drilling in the Western Pacific. In: Taylor, B., Natland, J. (Eds.), Active Margins and Marginal Basins of the Western Pacific. AGU Geophys. Mon., vol. 88. American Geophysical Union, Washington, DC, pp. 1–30.

Brown, D., Spadea, P., 1999. Processes of forearc and accretionary complex formation during arc–continent collision in the southern Urals. Geology 27, 649–652.

Buchkovskiy, E.S., 1970. Sulphide mineralization connected with ultramafic intrusions of the Western part of Magnitogorskiy megasinform. Geology, Mineralogy and Geochemistry of South Urals Sulphide Deposits. Ufa Institute of Geology Publications, Ufa, pp. 114–135. In Russian.

Bulanova, G.P., 1995. The formation of diamond. J. Geochem. Explor. 53, 1–23.

Burkhard, D.J.M., 1993. Accessory chromium spinels: their coexistence and alteration in serpentinites. Geochim. Cosmochim. Acta 57, 1297–1306.

Candela, P.A., Wylie, A.G., Burke, T.M., 1989. Genesis of the ultramafic rock-associated Fe–Cu–Co–Zn–Ni deposits of the Sykesville District, Maryland Piedmont. Econ. Geol. 84, 663–675.

Dick, H.J.B., 1977. Partial melting in the Josephine peridotite: I. The effect on mineral composition and its consequence for geobarometry and geothermometry. Am. J. Sci. 277, 801–832.

Dick, H.J.B., Bullen, T., 1984. Chromite as a petrogenetic indicator in abyssal and alpine-type peridotites and spatially associated lavas. Contrib. Mineral. Petrol. 86, 54–76.

Goodfellow, W.D., Franklin, J.M., 1993. Geology, mineralogy, and chemistry of sediment-hosted clastic massive sulfides in shallow cores, Middle Valley, northern Juan de Fuca Ridge. Econ. Geol. 88, 2037–2068.

Groves, D.I., Barrett, F.M., Brotherton, R.H., 1983. Exploration significance of chrome-spinels in mineralised ultramafic rocks and nickel–copper ores. Geol. Soc. South Africa Spec. Publ. 7, 21–30.

Herrington, R.J., Armstrong, R.N., Zaykov, V.V., Maslennikov, V.V., Tessalina, S.G., Orgeval, J.-J., Taylor, R.N., 2002. Massive sulfide deposits in the South Urals: geological setting within the framework of the Uralide Orogen. In: Brown, D., Juhlin, C., Puchkov, V.N. (Eds.), Mountain Building in the Uralides. AGU Geophys. Monogr., vol. 132. American Geophysical Union, Washington, DC, pp. 155–182.

Hottin, A.-M., Aloub, O., 1990. Les chromites hydrothermales accompagnant les minéralisations sulfurées et aurifères du district d'Ariab (Red Sea Hills-Soudan). Chron. Rech. Min. 498, 15–27.

Johan, Z., 1986. Chromite deposits of New Caledonian ophiolitic nappes. In: Petrascheck, W., Karamata, S., Kravchenko, G.C., Johan, Z., Economou, M., Engin, T. (Eds.), Chromites. Theophrastus Publications, Athens, pp. 311–338.

Johan, Z., Dunlop, H., Le Bel, L., Robert, J.L., Volfinger, M., 1983. Origin of chromite deposits in ophiolite complexes: evidence for a volatile and sodium-rich reducing fluid phase. Fortschr. Mineral. 61, 105–107.

Johnson, R.W., Macnab, R.P., Arculus, R.J., Ryburn, R.J., Cooke, R.J.S., Chappell, B.W., 1983. Bamus volcano, Papua New Guinea: dormant neighbour of Ulawn, and magnesian-andesite locality. Geol. Rundsch. 72, 207–237.

Kamenetsky, V.S., Crawford, A.J., Meffre, S., 2001. Factors controlling chemistry of magmatic spinel: an empirical study of associated olivine, Cr-spinel and melt inclusions from primitive rocks. J. Petrol. 42, 655–671.

Lehman, J., 1983. Diffusion between olivine and spinel: application to geothermometry. Earth Planet. Sci. Lett. 64, 123–138.

Li, J.-P., O'Neill, H.St.C., Seifert, F., 1995. Subsolidus phase relations in the system $MgO–SiO_2–Cr–O$ in equilibrium with metallic Cr, and their significance for the petrochemistry of chromium. J. Petrol. 36, 107–132.

Lindsley, D.H., 1983. Pyroxene thermometry. Am. Mineral. 68, 477–493.

Maslov, V.A., Cherkasov, V.L., Tishenko, V.T., 1993. Stratigraphy and Correlation of Middle Palaeozoic Volcanic Complexes of Main Sulphide Bearing Areas of South Urals. Bashkirian Centre of RAS, Ufa. In Russian.

Melekestseva, I.Yu., Zaykov, V.V., Tesalina, S.G., Augé, T., 2001. Chromites in sulphide ores in ultramafic rocks of the Main Urals Fault. The Urals Mineralogical Collection, vol. 11. The Institute of Mineralogy, Miass, pp. 180–189. In Russian.

Nimis, P., Omenetto, P., Tesalina, S.G., Zaykov, V.V., Tartarotti, P., Orgeval, J.-J., 2003. Peculiarities of some mafic–ultramafic-hosted massive sulfide deposits from southern Urals. A likely forearc occurrence. 7th SGA Meeting Proceedings Volume, Athens. In press.

Novgorod, M.I., Dmitri, M.T., Tzepin, A.I., Verinnik, V.M., 1984. Zoned chromites of hydrothermal metasomatic origin. Isvestia Acad. CCCP, Geol. Ser. 2 (in Russian).

Pearce, J.A., van der Laan, S.R., Arculus, R.J., Murton, B.J., Ishii, T., Peate, D.W., Parkinson, I.J., 1992. Boninite and harzburgite from leg 125 (Bonin–Marian forearc): a case study of magma genesis during the initial stage of subduction. Proc. ODP, Sci. Res. 125, 623–659.

Prokin, V.A., Buslaev, F.P., 1999. Massive copper–zinc sulphide deposits in the Urals. Ore Geol. Rev. 14, 1–69.

Puchkov, V.N., 1997. Structure and geodynamics of the Uralian orogen. In: Burg, J.-P., Ford, M. (Eds.), Orogeny Through Time. Geol. Soc. Spec. Publ., vol. 121. Geophysical Society, London, pp. 201–236.

Roedder, E., 1984. Fluid Inclusions. Reviews in Mineralogy, vol. 12. Mineralogical Society of America, Washington, DC.

Savelieva, G.N., Sharaskin, A.Ya., Saveliev, A.A., Spadea, P., Gaggero, L., 1997. Ophiolites of the southern Uralides adjacent to the East European continental margin. Tectonophysics 276, 117–137.

Savelieva, G.N., Sharaskin, A.Ya., Saveliev, A.A., Spadea, P., Pertsev, A.N., Babarina, I.I., 2002. Ophiolites and zoned mafic–ultramafic massifs of the Urals: a comparative analysis and some tectonic implications. In: Brown, D., Juhlin, C., Puchkov, V.N. (Eds.), Mountain Building in the Uralides. AGU Geophysical Monograph, vol. 132. American Geophysical Union, Washington, DC, pp. 135–153.

Scarrow, J.H., Hetzel, R., Gorozhanin, V.M., Dinn, M., Glodny, J., Gerdes, A., Ayala, C., Montero, P., 2002. Four decades of geochronological work in the Southern and Middle Urals: a review. In: Brown, D., Juhlin, C., Puchkov, V.N. (Eds.), Mountain Building in the Uralides. AGU Geophysical Monograph, vol. 132. American Geophysical Union, Washington, DC, pp. 233–255.

Schiano, P., Clocchiatti, R., Shimizu, N., Maury, R.C., Jochum, K.P., Hofmann, A.W., 1995. Hydrous, silica-rich melts in the sub-arc mantle and their relationship with erupted arc lavas. Nature 377, 595–600.

Seravkin, I.B., Znaminsiy, S.E., Kosarev, A.M., 2001. Fault Tectonics and Ore Deposits of the Trans-Uralian Bashkiria. Poligrafcombinat, Ufa. In Russian.

Simonov, V.A., Zaykov, V.V., Kolmogorov, Yu.P., 2002. Geochemistry of basalts from the ophiolite and suture zones of the South Urals. Metallogeny of Ancient and Modern Oceans—2002. Forming and Exploitation of Deposits in Ophiolite Zones. Miass Institute of Mineralogy, UB RAS, Miass, pp. 17–26. In Russian.

Smith, D., Lindsley, D.H., 1971. Stable and metastable augite crystallization trends in a single basalt flow. Am. Mineral. 56, 225–233.

Spadea, P., Kabanova, L.Ya., Scarrow, J.H., 1998. Petrology, geochemistry, and geodynamic significance of mid-Devonian boninitic rocks from the Baimak–Buribai area (Magnitogorsk Zone, southern Urals). Ofioliti 23, 17–36.

Spadea, P., D'Antonio, M., Kosarev, A., Gorozhanina, Y., Brown, D., 2002. Arc–continent collision in the southern Urals: petrogenetic aspects of the forearc–arc complex. In: Brown, D., Juhlin, C., Puchkov, V.N. (Eds.), Mountain Building in the Uralides. AGU Geophysical Monograph, vol. 132. American Geophysical Union, Washington, DC, pp. 101–134.

Tessalina, S.G., Zaykov, V.V., Orgéval, J.-J., Augé, T., Omenetto, P., 2001. Mafic–ultramafic hosted massive sulphide deposits in Southern Urals (Russia). In: Piestrzynski, A., et al. (Eds.), Mineral Deposits at the Beginning of the 21st Century. Swets & Zeitlinger, Lisse, pp. 353–356.

Treloar, P.J., 1987. The Cr minerals of Outokumpu—their chemistry and significance. J. Petrol. 28, 867–886.

Tucker, R.D., Bradley, D.C., Ver Straeten, C.S., Harris, A.G., Ebert, R., McCutcheon, S.R., 1998. New U–Pb zircon ages and the duration of Devonian time. Earth Planet. Sci. Let. 158, 175–186.

Walker, D.A., Cameron, W.E., 1983. Boninite primary magmas: evidence from the Cape Vogel peninsula. PNG Contrib. Mineral. Petrol. 83, 150–158.

Whitney, J.A., Naldrett, A.J., 1989. Ore Deposition Associated with Magmas. Rev. Econ. Geol., vol. 4. Society of Economic Geologists, Chelsea, MI.

Wipfler, E.L., Buschman, B., Zaykov, V.V., 1999. The mafic–ultramafic-hosted massive sulphide deposit of Ishkinino, Southern Urals. In: Stanley, C.J., et al. (Eds.), Mineral Deposits: Processes to Processing. Balkema, Rotterdam, pp. 613–616.

Yumul Jr., G.P., Balce, G.R., 1994. Supra-subduction zone ophiolites as favorable hosts for chromitite, platinum and massive sulfide deposits. J. Southeast Asian Earth Sci. 10, 65–79.

Zakharov, A.A., Zakharova, A.A., 1975. The ore composition at the Ivanovka sulfide deposit in the southern Urals versus their relation to specific lithology of host rocks. Geologiya i Usloviya Obrazovaniya Mestorozhdenii Medi na Yuzhnom Urale (Geology and Conditions of Formation of Copper Deposits in the Southern Urals) Institute of Geology Publications, Ufa, pp. 100–105. In Russian.

Zaykov, V.V., Zaykova, E.V., Maslennikov, V.V., 2000a. Volcanic complexes and ore mineralization in spreading basins of the southern Urals. In: Mezhelovsk, N.V. (Ed.), Geodynamics and Metallogeny: Theory and Implications for Applied Geology. Ministry of Natural Resources of the RF and Geokart, Moskow, pp. 315–337.

Zaykov, V.V., Tesalina, S.G., Melekeszeva, I.Yu., Auge, T., Orgeval, J.-J., Tatarko, N.I., 2000b. Sulphide deposits among the ultramafic rocks of the Urals paleoocean. Metallogeny of Ancient and Modern Oceans—2000. Miass Institute of Mineralogy, UB RAS, Miass, pp. 53–57. In Russian.

Zaykov, V.V., Maslennikov, V.V., Zaykova, E.V., Herrington, R., 2002. Rudno-Formatsionnyi i Rudno-Fatsial'nyi Analiz Kolchedannykh Mestorozhdenii Ural'skogo Paleookeana (Ore-Formation and Ore-Facial Analysis of Massive Sulphide Deposits of the Urals Palaeoocean). Miass Institute of Mineralogy, UB RAS, Miass. In Russian.

Zierenberg, R.A., Koski, R.A., Morton, J.L., Bouse, R.M., 1993. Genesis of massive sulfide deposits on a sediment-covered spreading center, Escanaba Trough, southern Gorda Ridge. Econ. Geol. 88, 2069–2098.